Proc. Natl. Acad. Sci. USA
Vol. 78, No. 6, pp. 3678–3682, June 1981
Cell Biology

Crystalline arrays of membrane-bound acetylcholine receptor

(tubular structures/membrane proteins/electron microscopy/antibody labeling/image processing)

JOERG KISTLER AND ROBERT M. STROUD*

Department of Biochemistry and Biophysics, School of Medicine, University of California, San Francisco, California 94143

Communicated by Walther Stoeckenius, March 12, 1981

ABSTRACT **Electron micrographs of tubular structures with a crystalline arrangement of membrane-bound acetylcholine receptor oligomers have been analyzed by digital image reconstruction. The receptor molecules are oriented synaptic side out, and in projection they appear to be asymmetric and have a defined orientation. All four subunits are contained in the oligomers as demonstrated by immunoelectron microscopy; these structures therefore appear to be suitable for subunit localization in the oligomer.**

Acetylcholine receptor (AcChoR)-rich membranes isolated from electric fish electroplaques contain "rosette" structures 70–80 Å in diameter [identified as AcChoR molecules (1)] dispersed in the plane of the membranes when analyzed by negative-stain electron microscopy (1–7).

Image reconstructions of electron micrographs from either crystalline (4) or noncrystalline (7) arrangements of AcChoR show a characteristically asymmetric projection structure. In another case, crystalline arrangements of AcChoR have been interpreted as indicating 3- or 6-fold symmetry of the oligomer in projection (8). Because the molecule is funnel-shaped and extends 55 Å above the membrane surface on the synaptic side of the membrane (1, 4, 9), there are strong cylindrically symmetric harmonics at low resolution.

We have developed conditions that reproducibly lead to the formation of tubular membranous structures from isolated AcChoR membranes; these structures show a crystalline arrangement of receptor protein in a lipid bilayer matrix. The tubes are labeled with antibodies directed against each of the four different AcChoR subunit types (10), which demonstrates conclusively that the observed cylindrical arrays are made of AcChoR molecules containing all four subunit species. Digital image processing of electron micrographs from negatively stained AcChoR tubes reveals characteristic structural features of the AcChoR complex and further defines its orientation. The tubes thus appear to be suitable for future localization of individual subunit sites in the oligomer structure, information necessary for understanding AcChoR function.

MATERIALS AND METHODS

Membrane Preparation and Annealing. AcChoR-rich membrane fractions were prepared from frozen *Torpedo californica* electric organ by a modification of the procedure of Klymkowsky *et al.* (11) which emphasizes (*i*) minimization of endogenous proteolysis and (*ii*) soft-pelleting of the membranes and gentle resuspension by pipetting to preserve large membrane vesicles and membrane fragments.

For a standard membrane preparation, 60 g of frozen tissue was homogenized (Virtis homogenizer, 4 min at full speed) in 120 ml of ice-cold buffer A (400 mM NaCl/10 mM *N*-ethylmaleimide/5 mM EDTA/5 mM ethylene glycol bis(β-aminoethyl ether)*N,N,N',N'*-tetraacetic acid/0.1 mM phenylmethylsulfonyl fluoride/0.01% NaN_3/50 mM sodium phosphate, pH 7.4). After centrifugation (Sorvall SS34, 6000 rpm, 10 min) the supernatant was passed through eight layers of cheesecloth. The filtrate was centrifuged (Sorvall SS34, 18,000 rpm, 45 min) and the pellet was resuspended with a pipette in buffer B (1 mM EDTA/1 mM ethylene glycol bis(β-aminoethyl ether)*N,N,N',N'*-tetraacetic acid/0.1 mM phenylmethylsulfonyl fluoride/0.01% NaN_3/10 mM sodium phosphate, pH 7.4). One additional cycle of low speed/high speed centrifugation was performed before the pellet was resuspended in buffer B containing 26% (wt/wt) sucrose to make 2 ml of total sample. One-milliliter aliquots thereof were overlayered onto 28–40% (wt/wt) linear sucrose gradients in buffer B and centrifuged overnight in a Beckman SW 40 rotor at 30,000 rpm; 0.6-ml fractions were collected from the gradients. Samples were kept at 0–4°C throughout.

Gradient fractions were analyzed by $NaDodSO_4$ gel electrophoresis; three or four fractions with sucrose densities 35–37% and protein concentrations averaging 1.2 mg/ml revealed a protein pattern identical to the one shown in figure 2*a* of ref. 11 and designated "AcChR-rich membrane fractions." Electron microscopy of negatively stained AcChoR-rich membrane samples at this stage revealed predominantly membranes with dispersed rosette-like structures.

AcChoR-rich gradient fractions were annealed at 4°C and periodically analyzed for gross structural changes by electron microscopy. After approximately 6 weeks, all samples contained significant numbers of ordered tubular structures which increased in proportion of the total sample with time. These are the subject of this analysis.

Electron Microscopy. AcChoR-rich membrane fractions were adsorbed onto carbon/collodion-coated copper grids previously rendered hydrophilic by glow-discharge in an atmosphere of air at reduced pressure. Nonadsorbed membrane material was removed by floating the grids on several drops of distilled water. Specimens were negatively stained with 1% uranyl acetate and examined in a Philips 300 electron microscope operated at 80 kV with a 30-μm objective aperture and a liquid nitrogen anticontamination device. Micrographs were recorded on Kodak electron microscope film 4489 at a standard magnification of 41,000 (calibrated with the 27-Å meridional spacing of stacked disk aggregates of tobacco mosaic virus).

Antisera and Antibody Labeling. Ammonium sulfate precipitated antibodies from rabbit antisera (raised against purified AcChoR or specifically against each of its subunit species α, β, γ, δ) and from preimmune antisera were generously provided by M. Raftery and T. Claudio (10).

For antibody labeling of tubular AcChoR-structures, annealed membrane material (protein concentration, 0.2 mg/ml)

The publication costs of this article were defrayed in part by page charge payment. This article must therefore be hereby marked "*advertisement*" in accordance with 18 U. S. C. §1734 solely to indicate this fact.

Abbreviation: AcChoR, acetylcholine receptor.

* To whom reprint requests should be addressed.

was adsorbed onto carbon/collodion-coated copper grids for 2 min; nonadsorbed particles were removed by floating the grids on 20 mM phosphate (pH 7.4). Adsorbed structures were stabilized by crosslinking with 1% glutaraldehyde at pH 7.4 for 1 min; then the grids were floated on phosphate buffer to remove excess glutaraldehyde. Most of the liquid was drained from the grids with filter paper and the grids were floated on 20-μl droplets of antibody solution (20 mg/ml) for 1 hr at room temperature. Removal of nonspecifically adsorbed antibodies was achieved by floating the grids on 1 M NaCl in phosphate buffer. The grids were washed free of salt on several drops of distilled water and negatively stained with 1% uranyl acetate.

Image Processing. Electron micrographs of tubular AcChoR structures were analyzed by optical diffraction for selection of those that preserved the integrity of the two superimposed surface lattices of the flattened structures. Areas on selected micrographs were digitized with a Syntex AD-1 flatbed scanner, operating with a 32 × 32 μm spot size (12). Computer filtering of the two surface lattices of each tube was as described by Ross *et al.* (4).

RESULTS

Morphological Aspect of Fresh and Annealed AcChoR-Rich Membrane Preparations. Electron microscopy of standard (nonannealed) AcChoR-rich membrane preparations revealed that the major portion of membranes contain a high density of rosette-type structures (Fig. 1*A*) that are distinct from amorphous membrane material. These rosettes have been identified previously as individual molecules of membrane-bound AcChoR by immunoelectron microscopy (1).

Annealed AcChoR-rich membrane fractions uniformly revealed three predominant representative classes of structures. (*i*) Membrane sheets containing areas of closely packed, frequently ordered rosettes distinct from large rosette-free regions. (*ii*) Membrane sheets with regularly arranged rosettes that show a tendency to roll up into tubes (Fig. 1*B*); these structures are often associated with membrane areas containing unordered rosette clusters. (*iii*) Tubular structures up to 10,000 Å in length and about 1100 Å in width (Fig. 1 *C–E*). Optical diffraction patterns of these flattened cylindrical particles showed two lattices superimposed in a defined fashion. Single-layered tube ends revealed an ordered arrangement of rosettes (Fig. 1*C*). The proportion of sample that was tubular increased with annealing time. The structures described under *i* and *ii* seem to represent intermediates on the pathway to tube formation. There was no detectable proteolysis of subunits in any of the annealed samples.

Serological Characterization of AcChoR Tubes. Ordered structures in the annealed material were characterized by treatment with antibodies raised against whole AcChoR and against each of the purified subunit species of AcChoR complex and examination electron microscopically. To minimize crosslinking between AcChoR membrane fragments, the antibody labeling procedure was carried out on structures after adsorption onto the supporting film. Tubes that had reacted with antibodies obtained from nonimmunized animals retained a clearly visible latticed structure (Fig. 2*A*). Tubes were coated with anti-AcChoR antibodies, anti-α, anti-β, anti-γ, and anti-δ antibodies (Fig. 2 *B–F*).

These results demonstrate conclusively that the tubes are formed from AcChoR membranes and, further, contain all of the four subunit types present in AcChoR.

Structural Analysis of AcChoR Tubes. Negatively stained AcChoR tubes reveal a characteristic edge structure previously identified as the synaptic side of AcChoR membranes from toxin/antitoxin antibody labeling experiments (1). This fine structure

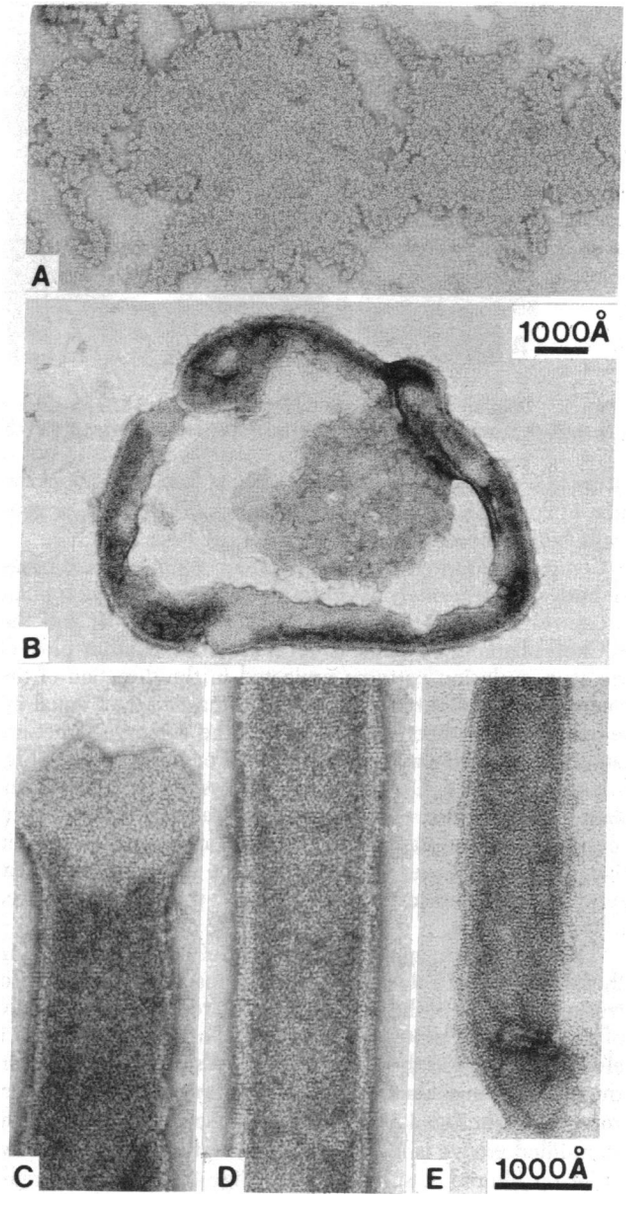

FIG. 1. AcChoR membrane structures from standard (*A*) and annealed (*B–E*) preparations, stained with 1% uranyl acetate. (*A*) Membrane sheet with dispersed AcChoR oligomers. (*B*) Membrane areas with ordered oligomer clusters exhibit tendency to role up. (*C–E*) Tubular AcChoR membranes; the ordered oligomer arrangement is revealed at the single-layered tube end in *C*.

resolved into doublets of protrusions, approximately 55 Å long, linearly arranged at regular intervals and corresponds to the projected side view of AcChoR. Thus, the AcChoR complexes in the tube membrane are oriented synaptic side out.

Optical diffraction patterns recorded from masked areas on micrographs of well-preserved negatively stained tubes typically showed reflections extending to about 30-Å resolution (Fig. 3*A*). All reflections can be indexed on two lattices, each of which derives from one side of the flattened tube (Fig. 3 *B* and *C*). Of the two lattices, one (the A lattice) always contained about 50–70% higher power in the reflections (Fig. 3*B*). The other (B lattice) always showed smaller real-space dimensions perpendicular to the tube axis (Fig. 3*C*). By analogy with the results of an extensive structural analysis of negatively stained T-even giant bacteriophages (13) and bacteriophage tail struc-

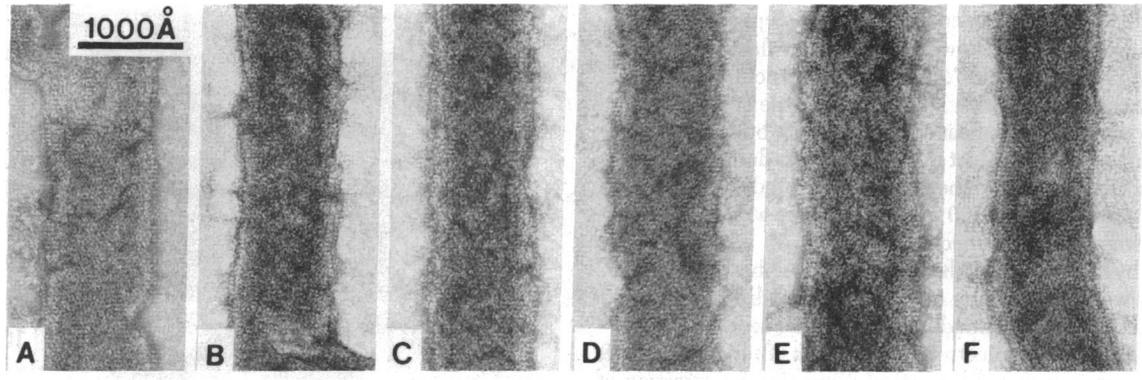

FIG. 2. Tubular structures stained with 1% uranyl acetate after reaction with antibodies as follows: *A*, preimmune; *B*, anti-AcChoR; *C*, anti-α; *D*, anti-β; *E*, anti-γ; *F* anti-δ. Note that the latticed structure of the tubes is obscured by the presence of bound antibodies in *B–F*.

tures (14), we suggest that the A lattice is from the side of the tube in contact with the hydrophilic support film and is generally better preserved.

Computer filtering was carried out for seven selected tubes for both sides separately. As examples, filtrations of the tubular structures in Fig. 1 *D* and *E* are shown in Fig. 4, and the AcChoR oligomer structure is represented as contour plots of the stain exclusion patterns projected in the direction of the electron beam. Contour levels in the images are at equal intervals and have been chosen so that the common structural features are prominantly represented. For the A surface (Fig. 4 *A* and *B*) the AcChoR oligomer shows three predominant stain-excluding areas corresponding to peaks in the protein surrounding a central stain-penetrated well approximately 20 Å in diameter at the bilayer surface. One of the stain-excluding areas represents a significantly smaller protein protrusion compared to the two others.

The asymmetric appearance of the AcChoR complex is further enhanced by a stain-filled groove separating the small protrusion from one of the larger ones. The respective orientation of groove, small protrusion, and the two large protrusions is always clockwise in the A lattice. If the A surface lattice is from the tube side in contact with the supporting film, then the view represented in Fig. 4 *A* and *B* is from the cytoplasmic side. The stain-filled groove is in the left-handed lattice direction in five of seven filtered A surfaces (as in Fig. 4*A*) but in the right-handed lattice direction it is in the two others (as in Fig. 4*B*).

This difference indicates polymorphism in the tube folding rather than a filtering artifact for the following reasons. (*i*) The respective orientation of the structural features in the AcChoR oligomer projection is identical in all tubes; thus, the lattice as a whole appears rotated by about 120° in the less-frequent shape. (*ii*) For most tubes, the direction of the stain-filled groove in the filtered A surface has been verified with the filtration of the respective B surface, from the other side of the tube in which the major groove appears to be flipped over the tube axis (Fig. 4*C*). Reconstructed images from the more distorted B surface are more variable than those from the A surface and the oligomers are compressed equatorially, presumably due to distortions of exactly the kind discussed by Moody (14). (*iii*) The lattice dimensions and tube diameter differ between the two classes of tubular structures. One lattice vector (designated *a*) is always parallel ($\pm 0.8°$, $n = 7$) to the tube axis. For the class of tubular structures that have the stain-filled groove approximately 60° counterclockwise from *a* on the A surface (Fig. 4*A*), the *a* cell dimension is 92 ± 2.2 Å ($n = 5$) and is identical ($\pm 0.8\%$) for both sides of each tube. For the A surface, the *b* cell dimension ($\gamma = 125 \pm 2°$ clockwise from the *a* axis) is 85 ± 1.7 Å. On the equatorially contracted B surface, the *b* cell dimension ($\gamma = 132 \pm 3°$ counterclockwise from *a*) is 75.1 ± 3.9 Å. With the relatively consistent width of the flattened tubes (1200 ± 70 Å outside diameter), their structure is described as right-handed, two-start helix with a pitch of 90 ± 4 Å and 19 ± 1 AcChoR molecules encircling the tube in the direction inclined about 5° to the equator.

The second class of tubular lattices in which the groove is approximately 60° clockwise from the tube axis on the A surface (Fig. 4*B*) shows significantly shorter lattice dimensions (84.5 ± 0.5 Å parallel to the tube axis), approximately 20% smaller unit cell area, and smaller tube width (1013 ± 60 Å outer di-

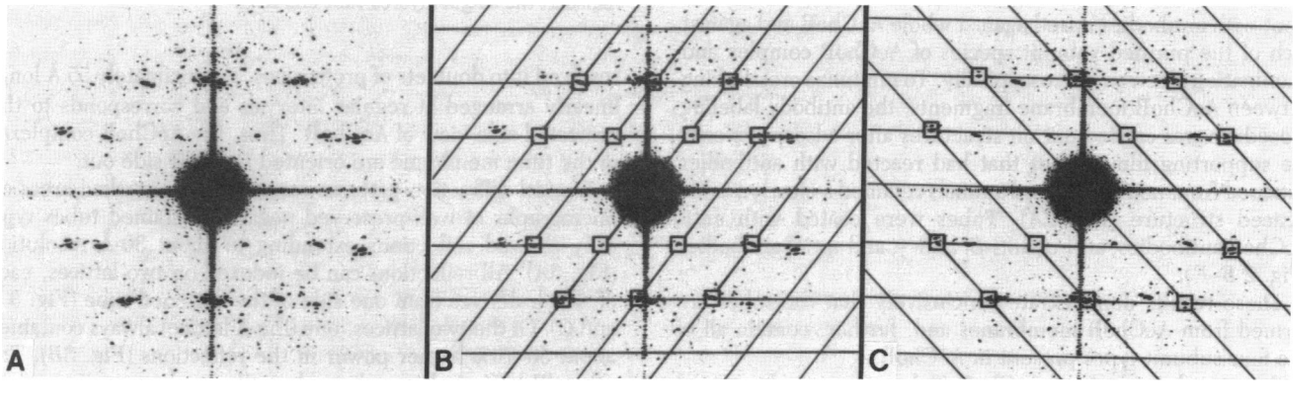

FIG. 3. Optical diffraction pattern recorded from a rectangular stretch of the tubular structure in Fig. 1*E*; tube axis is vertical. (*A*) Original diffraction pattern containing reflections from both sides of the flattened tube. (*B*) Indexation for lattice A. (*C*) Indexation for lattice B. Lattice A is most likely derived from the structurally better preserved tube side in contact with the support.

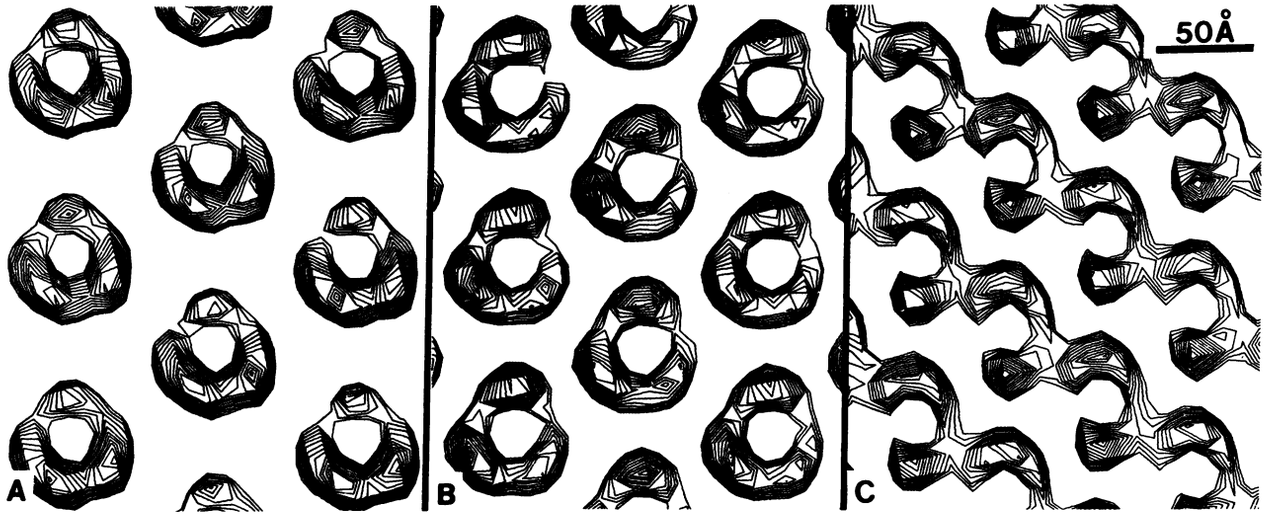

FIG. 4. Filtered projection views of membrane-bound AcChoR oligomers displayed as density contour maps. (*A*) Reconstructed from the structurally better preserved A surface of the tube in Fig. 1*D*. The stain-filled groove faces to the left for five of seven tubes. (*B*) Reconstructed from the A surface of the tube in Fig. 1*E*. The groove faces to the right for two of seven tubes. (*C*) Reconstructed from the more distorted B surface of the tube in Fig. 1*E*. All images are oriented such that the tube axis is vertical. The *a* lattice direction is always parallel to the tube axis; the *b* lattice direction is 125°clockwise from *a* in *A* and *B* and is 132° counterclockwise from *a* in *C*.

ameter). The pitch and number of molecules per turn in the right-handed helix remains the same. Thus, molecules pack together more closely when curved around the shorter cell axis—i.e., the $a + b$ direction in Fig. 4*A*.

DISCUSSION

AcChoR Tube Oligomer Structure. AcChoR occurs both as a 250,000-dalton monomer and as a dimer crosslinked by a disulfide bond between the δ subunits (15, 16). Electron micrographs of membranes reconstituted from lipid and solubilized AcChoR that was predominantly dimeric revealed a corresponding proportion of distinct double rosettes and few single rosettes (data not shown). Thus, each of the rosettes contoured in Fig. 4 *A* and *B* represents the projection view of a single AcChoR monomer.

Approximately 70% of the δ subunits were crosslinked δ_2 dimers in AcChoR membrane preparations which yielded tubes upon annealing. Yet, filtered images of tubular particles reveal an apparently unique oligomer orientation and there is no semblance of a 2-fold axis between molecules. Reduction to monomer in the annealed membrane sample did not alter the appearance of the tubes. Furthermore, structure analysis of small ordered planar arrays of membrane-bound AcChoR showed no difference between preparations rich in monomeric compared to dimeric AcChoR (unpublished data). Thus, ordered AcChoR membrane lattices may selectively form from monomeric AcChoR alone. Dimers may account for the unordered rosette clusters often found associated with intermediates in tube assembly (Fig. 1*B*). Alternatively, two oligomers may be crosslinked via a flexible loop on the δ subunit, which might also allow for the unique oligomer orientation in the filtered tube images. We have not yet succeeded in separating the tubular structures from the other material in the annealed membrane fraction, which is desirable for further characterization of chemical differences between different parts of the sample.

The AcChoR complex protrudes by 55 Å above the synaptic surface and by 15 Å on the cytoplasmic side (1, 4). Thus, the stain-exclusion patterns displayed in Fig. 4 predominantly represent the tube outside—i.e., the projection of the membrane synaptic surface topography. Contact zones between oligomers in the tubular lattice are situated close to or within the lipid bilayer because protruding components of the AcChoR molecules are compressed in the flattened B surface in the equatorial direction. Contoured to lower densities than in Fig. 4 *A–C*, features in the contact regions are very low and mainly due to noise, supporting this conclusion.

The oligomer structure presented here is similar to that derived from the less distorted one of the two superimposed planar crystalline arrays of membrane-bound AcChoR represented in figures 8*a* and 9*a* in ref. 4. The contrast variation around the AcChoR rosette is consistent with that expected for the different sizes of the subunits. Averaging of randomly dispersed AcChoR oligomers by correlation techniques (7) has therefore been possible and also has given rise to a somewhat similar projection view, although the averaged oligomer orientations are poorly defined due to similarity of the three main maxima. The structure of the AcChoR complex is not consistent with a 6-fold or with a 3-fold symmetric oligomer structure concluded from image analysis of tubular structures somewhat similar in aspect to ours (8).

Subunit Localization in AcChoR Oligomer Structure. The asymmetric shape of the AcChoR complex derived from the tubes reflects the asymmetry in the subunit composition $\alpha_2\beta\gamma\delta$ (17–19). All subunits span the phospholipid bilayer (20). The molecule also contains α-helices up to 80 Å long and oriented perpendicular to the membrane (4). Circular dichroism indicates that 34% of AcChoR is α-helical (21). We suggest that all subunits are elongated perpendicular to the membrane and are arranged around the central ionophoretic channel much as five staves of a barrel. In this global model the variation in molecular weight determines the height of each subunit perpendicular to the membrane plane and thus contrast in the image. In the simplest view, the three main maxima in the projected AcChoR oligomer structure could be assigned to the β, γ, and δ subunits, and the two α subunits would be located at minima between protein peaks.

In a more complex case, stain-exclusion domains in the filtered image might be due to contributions from more than one subunit. A feasible approach for the solution of the subunit arrangement in the AcChoR oligomer involves image reconstruc-

tion of tubes labeled with subunit-specific antibodies. This approach has already been successfully applied to bacteriophage T4 giant heads (22) and polyheads (23). Two criteria were found to be important. (*i*) Labeling with Fab fragments is preferred to labeling with whole antibodies because of smaller size and monovalent binding nature. (*ii*) Fab fragments attached to the outside surface of cylindrical particles cause far less lattice distortion upon specimen preparation for electron microscopy than do Fab fragments bound to the inside surface. The cytoplasmic side of AcChoR membranes (the inside surface of the tubes) indeed reveals only faint antigenicity with respect to the synaptic 55-Å protruding component of the AcChoR complex (24).

Note Added in Proof. After this manuscript was submitted, Karlin and coworkers (25) reported that, for AcChoR solubilized in Triton X-100, the "rosette" structure is due to the receptor monomer and that the δ_2 crosslinked dimer is represented by two connecting rosettes in negatively stained specimens. Our analysis of the morphological correlates of receptor monomers and dimers, briefly described in the first paragraph of the *Discussion*, has led to the same conclusion; however, our results have been obtained for AcChoR molecules dispersed in the membrane. Micrographs of widely dispersed membrane-bound AcChoR molecules will be published elsewhere (26).

We thank Drs. M. A. Raftery and T. Claudio for provision of antibodies, Dr. J. Lindstrom for useful discussion and provision of monoclonal antibodies, Dr. D. A. Agard for advice on image processing, and Drs. R. Fairclough, S. B. Hayward, U. Aebi, A. Steven, and D. A. Agard for critical readings of the manuscript. This work was supported by National Science Foundation Grant PCM80-21433, by National Institutes of Health Grant GM24485, and by a Swiss National Science Foundation Postdoctoral Fellowship to J.K.

1. Klymkowsky, M. W. & Stroud, R. M. (1979) *J. Mol. Biol.* **128**, 319–334.
2. Nickel, E. & Potter, L. T. (1973) *Brain Res.* **57**, 508–517.
3. Cartaud, J., Benedetti, E. L., Cohen, J. B., Meunier, J. C. & Changeux, J. P. (1973) *FEBS Lett.* **33**, 109–113.
4. Ross, M. J., Klymkowsky, M. W., Agard, D. A. & Stroud, R. M. (1977) *J. Mol. Biol.* **116**, 635–659.
5. Schiebler, W. & Hucho, F. (1978) *Eur. J. Biochem.* **85**, 55–63.
6. Cartaud, J., Benedetti, E. L., Sobel, A. & Changeux, J. P. (1978) *J. Cell Sci.* **29**, 313–337.
7. Zingsheim, H. P., Neugebauer, D. C., Barrantes, F. J. & Frank, J. (1980) *Proc. Natl. Acad. Sci. USA* **77**, 952–956.
8. Brisson, A. (1978) in *Proceedings of the Ninth International Congress on Electron Microscopy*, Toronto, ed. Sturgess, J. M. (Imperial, Mississauga, ON, Canada), Vol. 2, pp. 180–181.
9. Stroud, R. M. & Agard, D. A. (1979) *Biophys. J.* **25**, 495–512.
10. Claudio, T. & Raftery, M. A. (1977) *Arch. Biochem. Biophys.* **181**, 484–489.
11. Klymkowsky, M. W., Heuser, J. E. & Stroud, R. M. (1980) *J. Cell Biol.* **85**, 823–838.
12. Ross, M. J. & Stroud, R. M. (1977) *Acta Crystallogr.* **33**, 500–508.
13. Aebi, U., Bijlenga, R. K. L., ten Heggeler, B., Kistler, J., Steven, A. C. & Smith, P. R. (1976) *J. Supramol. Struct.* **5**, 475–495.
14. Moody, M. F. (1971) *Philos. Trans. R. Soc. London Ser. B* **261**, 181–195.
15. Reynolds, J. A. & Karlin, A. (1978) *Biochemistry* **17**, 2035–2038.
16. Hamilton, S. L., McLaughlin, M. & Karlin, A. (1979) *Biochemistry* **18**, 155–163.
17. Lindstrom, J., Merlie, J. & Yogeeswaran, G. (1979) *Biochemistry* **18**, 4465–4470.
18. Raftery, M. A., Hunkapiller, M. W., Strader, C. D. & Hood, L. E. (1980) *Science* **208**, 1454–1457.
19. Karlin, A. (1980) in *The Cell Surface and Neuronal Function*, eds. Cotman, C. W., Poste, G. & Nicolson, G. L. (Elsevier/North-Holland, Amsterdam), pp. 191–260.
20. Strader, C. B. D. & Raftery, M. A. (1980) *Proc. Natl. Acad. Sci. USA* **77**, 5807–5811.
21. Moore, W. M., Holladay, L. A., Puett, D. & Brady, R. N. (1974) *FEBS Lett.* **45**, 145–149.
22. Aebi, U., ten Heggeler, B., Onorato, L., Kistler, J. & Showe, M. K. (1977) *Proc. Natl. Acad. Sci. USA* **74**, 5574–5578.
23. Kistler, J., Aebi, U., Onorato, L., ten Heggeler, B. & Showe, M. K. (1978) *J. Mol. Biol.* **126**, 571–589.
24. Strader, C. B. D., Revel, J. P. & Raftery, M. A. (1979) *J. Cell Biol.* **83**, 499–510.
25. Wise, D. S., Schoenborn, B. P. & Karlin, A. (1981) *J. Biol. Chem.* **256**, 4124–4126.
26. Kistler, J., Stroud, R. M., Klymkowsky, M. W., Lalancette, R. & Fairclough, R. H. (1982) *Biophys. J.*, in press.